Analysis Strategy – Overview

The event-selection process is two-staged, and contains:

1. The hardware-level trigger decision, based on calorimeter energy deposits in the bunch-crossings (BCs) $N-1$ and N.
2. Additionally for BC N, the software-based high-level trigger decision (similar to what the CalRatio 2022 analysis is doing) and the offline reconstruction.

1 Hardware Trigger

The hardware-based trigger exploits energy deposits in the calorimeters (ECAL and HCAL). To make a trigger decision within the available time, the hardware-based trigger uses a finite granularity/resolution. The calorimeter cells are summed to so-called trigger towers (TTs), which are typically[1] (0.1×0.1) in $(\eta \times \varphi)$, with only two layers (ECAL and HCAL) per TT.

Trigger Towers in MC Truth

In MC, all detector-stable truth particles that are visible in the calorimeters[a], and that are produced either in the trackers, ECAL, or HCAL, are assigned to the corresponding TT based on their (η, φ) coordinates *in the calorimeter*; i.e. **(i)** particles produced *inside the tracker*, at $(\vec{r}_0, t_0)$ with $\rho_0 = \sqrt{x_0^2 + y_0^2} < \rho_{\text{Calo}} = 1.4\,\text{m}$ and $z_0 < z_{\text{Calo}} = 3.7\,\text{m}$, need to be extrapolated [1, 2] to their calorimeter entry. For this, we use a simplified ATLAS calorimeter geometry as shown in Figure 1, and approximate the calorimeter entry linearly as visualised in Figure 2:

$$\vec{r}(t) = \vec{r}_0 + \vec{v} \cdot t \quad \text{with } \vec{v} = \vec{p}/E, \tag{1}$$

with t referring to the time of travel starting at $t = 0$ from $\vec{r}_0$. The calorimeter entry is obtained by solving $\rho(t) = \sqrt{x^2(t) + y^2(t)} = \rho_{\text{Calo}}$ and $z(t) = z_{\text{Calo}}$. These equations could give up to 3 solutions, from which the lowest positive real solution is the travel time (=: t_1) from the production vertex, $\vec{r}_0$, to the calorimeter entry, $\vec{r}_{\text{entry}} = \vec{r}(t_1)$. Subsequently, the η and φ coordinates could be calculated by

$$\eta = 1/2 \times \log\left(\frac{|\vec{r}_{\text{entry}}| + z_{\text{entry}}}{|\vec{r}_{\text{entry}}| - z_{\text{entry}}}\right) \quad \text{and} \quad \varphi = \text{atan2}(y_{\text{entry}}, x_{\text{entry}}). \tag{2}$$

For **(ii)** particles produced *within the ECAL or HCAL*, no extrapolation is needed, and the (η, φ) coordinates can directly be obtained by substituting the $\vec{r}_{\text{entry}}$ coordinates in (2) by the production vertex position, $\vec{r}_0$.
Particles produced within the trackers or the ECAL ($\rho_0 < 2\,\text{m}$ and $z_0 < 4.3\,\text{m}$) are assigned to the corresponding ECAL TTs, whereas particles produced in the HCAL are assigned to the corresponding HCAL TTs. Particles produced outside the calorimeters ($\rho_0 > 3.5\,\text{m}$ or $z_0 > 5.5\,\text{m}$) are not assigned to any TT.

[a] i.e. all particles except neutrinos, muons, and the BSM particles.

The hardware based calorimeter trigger uses typically energy deposits within a certain BC N, but in our case the energy deposits of the previous BC $N-1$ are additionally considered for the trigger decision. This allows us to study correlations between two time windows, namely 0 to 10 ns (the sensitive time window of $N-1$), and 25 to 35 ns (the sensitive time window of N), where $t = 0$ is defined at the pp collision in $N-1$. Here, the quoted times refer to the *synchronised readout-time*, which is the actual time, t, corrected by the "time-of-flight", tof:

[1] The TT size in η is slightly larger in the forward region, $|\eta| > 2.5$.

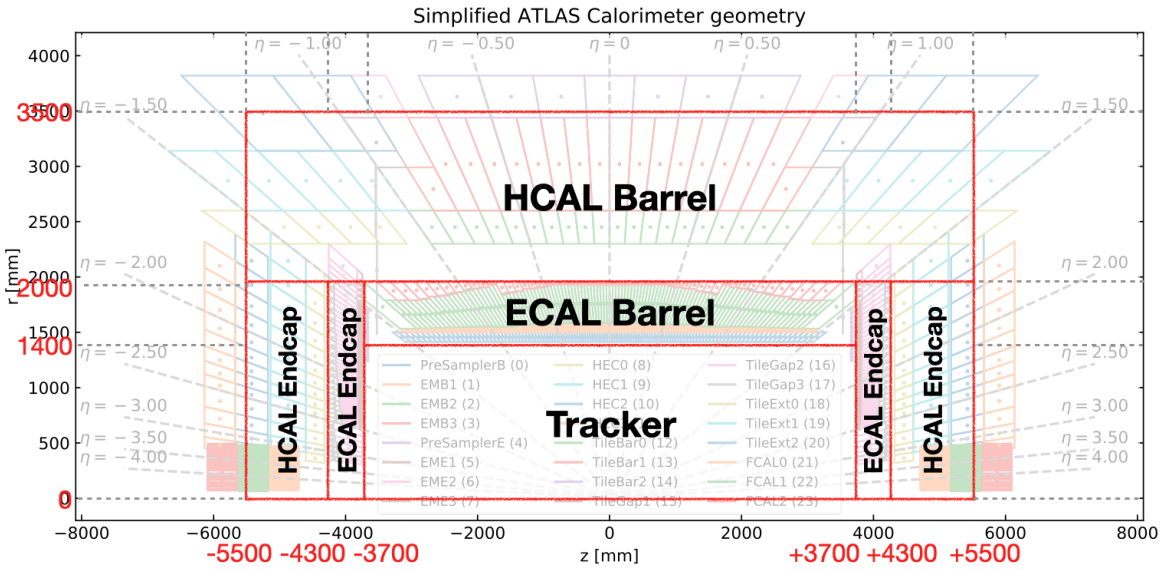

Figure 1: Simplified ATLAS geometry in the (ρ, z) plane. Figure modified from [8].

Synchronised Readout Time in MC Truth

The calorimeter timing is synchronised with the LHC clock, and the readout-time of a certain event (e.g. particle production/decay) is corrected for its "time-of-flight", $t_{\text{readout}} = t - \text{tof}$. All detector-stable truth particles (which are visible in the calorimeters) are assigned to the corresponding time window **(i)** based on their production vertex $(\vec{r}_0, t_0)$ if they are produced in the ECAL or HCAL, and **(ii)** based on the extrapolated calorimeter entry $(\vec{r}_{\text{entry}}, t_{\text{entry}})$ if they are produced in the trackers. The readout time is then approximated by

$$(i) \quad t_{\text{readout}} = t_0 - \frac{|\vec{r}_0|}{c}, \tag{3}$$

$$(ii) \quad t_{\text{readout}} = t_0 - \frac{|\vec{r}_0|}{c} + t_1 - \frac{|\vec{r}_{\text{entry}} - \vec{r}_0|}{c}. \tag{4}$$

Here, the first term in (ii) accounts for the travel from the interaction point to the production vertex, whereas the latter term accounts for the travel from the production vertex to the calorimeter entry. The readout time of particles produced outside the calorimeters could be set to infinity. In all cases, t_{readout} is used to assign the truth particles to the corresponding time windows (either $N-1$, N, or none of both).

Trigger Strategy

The hardware trigger is searching for a small radius jet ($R = 0.4$) in BC N exceeding an E_T threshold of 40 GeV (the definition of a jet in the context of the hardware trigger is given below). If BC N contains such a jet (in fact, the six most energetic jets in $|\eta| < 3.2$ are considered), the hardware trigger investigates whether BC $N-1$ did contain missing transverse energy (MET definition is also provided below) correlated in φ (i.e. $\Delta\varphi$ between the jet and MET is smaller than 1.0). If these conditions are fulfilled, the BC N is further processed by the software-based high-level trigger as described in the next section, and potentially readout for offline analysis.

Small R Jets

The jet algorithm in the hardware-based calorimeter trigger contains the following steps:

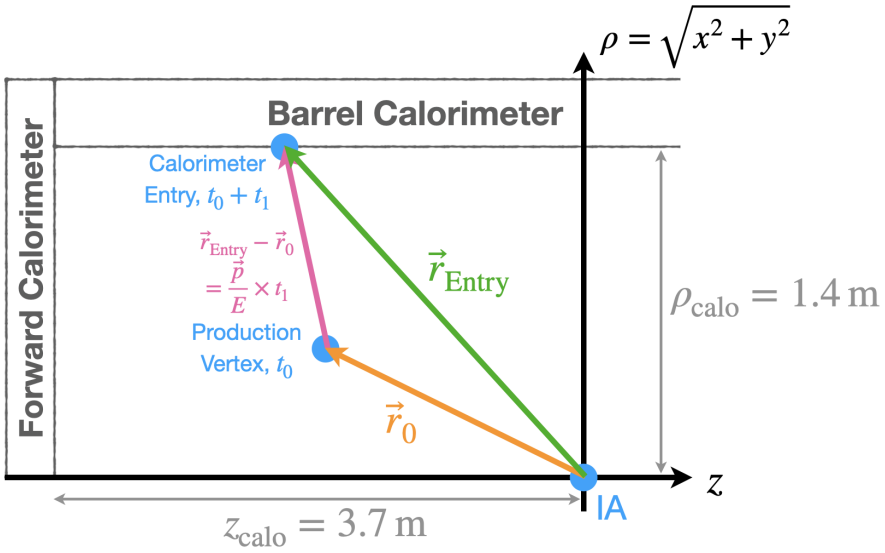

Figure 2: Visualisation of the extrapolation process in the $\rho \times z$ plane. In this example, a particle is produced displaced at $(\vec{r}_0, t_0)$ within the tracker, with a momentum $\vec{p}$. After a travel distance $|\vec{r}_{\text{Entry}} - \vec{r}_0|$ and a travel time t_1, it enters the calorimeter at $\vec{r}_{\text{Entry}}$ at the time $t_0 + t_1$. The readout time at the calorimeter entry is given by $t_0 + t_1 - \frac{|\vec{r}_0| + |\vec{r}_{\text{Entry}} - \vec{r}_0|}{c}$. The (η, φ) coordinates are defined by $\vec{r}_{\text{Entry}}$ rather than $\vec{p}$ which allows to assign the particle to the corresponding TT.

1. Only consider TTs that exceed a so-called noise cut (basically an energy threshold to exclude noise). TTs below the noise-cuts are assigned an energy of zero. These noise cuts are of the order of few GeV, they are η dependent, and in general distinct for the ECAL and HCAL TTs.

2. Search for local energy maxima. For each TT in $\eta \times \varphi$, the energy of the corresponding ECAL and HCAL TTs are summed; subsequently, each TT is considered as central seed of a 5×5 search window (5×5 TTs correspond to roughly 0.5×0.5 in $\eta \times \varphi$). The energies of the $5 \times 5 = 25$ TTs within each search window are summed, and thereafter compared (in a so-called sliding window algorithm) to the 24 neighbouring search windows (those search windows with central seed in any of the 24 neighbouring TTs of the original search window's central TT). A local maximum is found when the energy in the original search window is larger than in the 24 neighbouring search windows.

3. Sum energy of neighbouring TTs in a 9×9 window[2] around the central seed to form a $R = 0.4$ cone. Again, the sums of the ECAL and HCAL layer are taken here. Eventually, the jet E_T is estimated based on the η of the central seed, and the summed energy: $E_T = E/\cosh\eta$.

[2]In order to mimic an $R = 0.4$ circular shape, the edges of the 9×9 window are *not* considered, and also the corners of the remaining 8×8 window are not considered in the sum. The pattern is depicted in Figure 3.

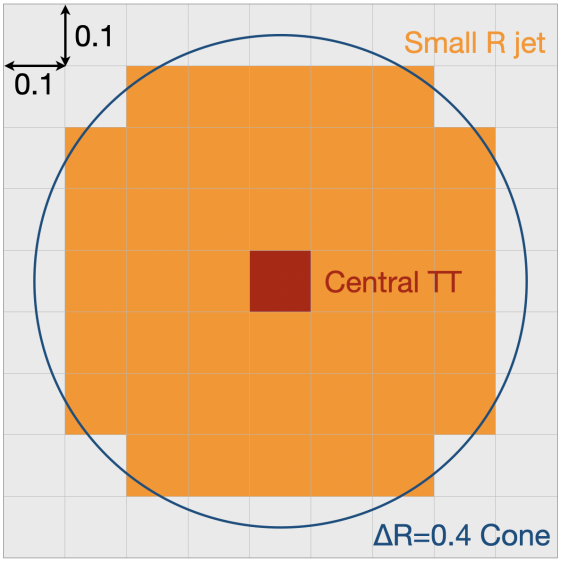

Figure 3: Visualisation of the shape of a small R jet in the $\eta \times \varphi$ plane.

Hardware Trigger jet in BC N in MC Truth

Based on equations (1) to (4), all particles in the readout time-window N within the ECAL and HCAL TTs are considered in the jet algorithm [3].

1. First, the TTs are compared (individually for the ECAL and HCAL layers) to the corresponding noise cuts, by summing the energies of all truth particles assigned to the individual TTs. Either the energy sum (if above the noise cut) is stored or the energy is set to zero (in case the energy sum is below the noise cut).

2. After summing the ECAL and HCAL layers, we loop over all 66×64 TTs in $\eta \times \varphi$ and compare their energy, E_{central}, to the 24 neighbouring TTs in a 5×5 TT window. Note that the sliding window algorithm has been simplified, by just comparing the central TT instead of the complete search windows. If the energy in the central TT is greater than the energies in all 24 neighbouring TTs, the central TT is stored as a local maximum.

3. Looping over all local maxima, the jet energies are computed by summing the corresponding TTs according to the circular shape in the 9×9 window. The jet η is taken from the central TT, and the transverse energy of the jet is calculated as $E_T = E/\cosh\eta$. The six most energetic jets in $|\eta| < 3.2$ are stored.

MET

The missing transverse energy at (hardware) trigger level is calculated by summing up the TT energies (weighted by $\sin\varphi$ and $\cos\varphi$) and calculating the energy balance (and computing the transverse part of it). In order to exclude noise, the individual TTs need to exceed a so-called noise-cut (basically an energy threshold), to be considered in the energy balance. TTs below the noise-cuts are assigned an energy of zero. These noise cuts are of the order of few GeV, they are η dependent, and in general distinct for the ECAL and HCAL TTs.

Hardware Trigger MET of BC $N-1$ in MC Truth

Based on equations (1) to (4), all particles in the readout time-window $N-1$ within the ECAL and HCAL TTs are considered for the MET calculation [4]. For each individual TT, the energies of all particles are summed, and compared to the corresponding noise-cut. In case the energy sum is below the noise-cut, the energy and momentum of this TT are set to 0, otherwise we set the momenta of TT J to

$$p^J_{x,y} = \sum_{i=0}^{N} p^i_{x,y}, \tag{5}$$

with i running over the corresponding truth particles in TT J. The energy balance is computed by summing over all TTs:

$$P_{x,y} = \sum_{J=0}^{2\times66\times64} p^J_{x,y} \tag{6}$$

where j is running over the 2 (ECAL and HCAL) $\times$ 66 (in η) $\times$ 64 (in φ) TTs. Subsequently, MET and φ calculated according to

$$\not{E}_T = \sqrt{P_x^2 + P_y^2} \quad \text{and} \quad \varphi = \text{atan2}(-P_y, -P_x). \tag{7}$$

Correlation between Jet and MET

To reduce the rate of our hardware-level trigger, a $\Delta\varphi$ correlation between the MET in $N-1$ and the jet in N is required: $\Delta\varphi(\text{MET}, \text{jet}) < 1.0$.

Hardware Level Trigger Decision of $N-1$ and N in MC Truth

In summary, the hardware-based trigger decision [5] requires:

- The MET object in $N-1$ must exceed the E_T threshold of 40 GeV, but be relatively soft (lower than $\sim 100\,\text{GeV}$) – otherwise a MET trigger would fire in $N-1$.
- At least one jet is required within $|\eta| < 3.2$ in N, with a threshold of 40 GeV.
- The $\Delta\varphi$ separations between the MET object (7) and any of the six most energetic jets are calculated. At least one jet with $\varphi(\text{MET}, \text{jet}) < 1.0$ (and E_T, η as defined above) is required. The most energetic jet with $\varphi < 1.0$ is denoted leading jet.

2 Software Trigger and Offline Reconstruction

After the hardware based trigger has found a correlation between BCs $N-1$ and N, BC N is further processed by the software-based high-level trigger. The cutflow at this stage is pretty similar to the CalRatio analysis, i.e. an isolated jet with a low fraction of energy deposit in the ECAL is required. In particular, at least one jet with

- $p_T > 20\,\text{GeV}$ and $|\eta| < 2.5$,
- $\text{EMF} = \frac{E_{\text{EM}}}{E_{\text{EM}}+E_{\text{HAD}}} < 0.06$, and
- $\Delta R(\text{jet,tracks}) > 0.2$ for tracks with $p_T > 2\,\text{GeV}$

is required. At the software-based high-level trigger, jets are close to what we know from offline jets, in our case $R = 0.4$ jets clustered with the AntiKt algorithm (without using particle flow algorithms).

High Level Trigger Decision of N in MC Truth (I)

We use truth jets clustered with the AntiKt algorithm with $R = 0.4$ to mimic the high-level trigger decision [6]. For each jet with $p_T > 20\,\text{GeV}$, we use the jet constituents (i.e. all detector stable truth particles contained in that jet) and their individual production vertices, in order to approximate the jet origin, which is used to assign the jets to the correct time window, and find the (η, φ) coordinates of the jet. Therefore, the production vertices of all jet constituents are first sorted based on their time, and subsequently the first vertex in this list, $(\vec{r}_0, t_0)$, with momentum fraction[a] $\frac{p_T(\text{vertex})}{p_T(\text{jet})} > 0.3$ is defined as the jet origin[b]

$$t_{\text{readout}} = t_0 - \frac{|\vec{r}_0|}{c}, \quad \eta = 1/2 \times \log\left(\frac{|\vec{r}_0| + z_0}{|\vec{r}_0| - z_0}\right), \quad \varphi = \text{atan2}(y_0, x_0). \tag{8}$$

Only jets in the time window N (i.e. $25 < t_{\text{readout}}/\text{ns} < 35$) with $|\eta| < 2.5$ are processed further, and have to pass the EMF and isolation cuts:

1. We approximate the EMF cut ($E_{EM} < 6.4\% E_{HAD}$), by checking if the jet is originating at most one interaction length away from the HCAL boundary: From Figure 4, we know the material budget (in units of hadronic interaction length) at the entry (λ_{entry}) and at the exit (λ_{exit}) of the ECAL as a function of $|\eta|$. We can use this to estimate the "remaining" interaction length [7], $\lambda_{\text{remaining}}$, which accounts for the material between the production vertex and the ECAL exit:

$$\frac{\lambda_{\text{exit}} - \lambda_{\text{entry}} - \lambda_{\text{remaining}}}{\lambda_{\text{exit}} - \lambda_{\text{entry}}} = \frac{d - d_{\text{remaining}}}{d}, \tag{9}$$

$$\Rightarrow \lambda_{\text{remaining}} = (\lambda_{\text{exit}} - \lambda_{\text{entry}}) \times \frac{d_{\text{remaining}}}{d} \tag{10}$$

with d being the thickness of the ECAL, and $d_{\text{remaining}}$ being the distance from the production vertex to the calorimeter exit:

$$d = \begin{cases} \dfrac{\rho_{\text{exit}} - \rho_{\text{entry}}}{\sin\theta} & |\eta| < 1.37 \\ \dfrac{z_{\text{exit}} - z_{\text{entry}}}{\cos\theta} & |\eta| > 1.70 \\ (1-\alpha)\left(\dfrac{\rho_{\text{exit}} - \rho_{\text{entry}}}{\sin\theta}\right) + \alpha\left(\dfrac{z_{\text{exit}} - z_{\text{entry}}}{\cos\theta}\right) & \text{else} \end{cases} \tag{11}$$

$$\text{with } \alpha = \frac{|\eta| - 1.37}{1.70 - 1.37}. \tag{12}$$

Here, the first case corresponds to the barrel region, the second case to the endcap region, and the third case to the transition region, where the jet travels through the barrel and the endcap. A similar expression for $d_{\text{remaining}}$ is obtained by substituting $(\rho_{\text{entry}}, z_{\text{entry}})$ by the production vertex coordinates (ρ_0, z_0). This allows to calculate the remaining interaction length (which is required to be less than 1):

See next page

[a] The numerator in this fraction also contains the p_T of particles originating from that vertex, but *not* clustered to the jet, which allows for values greater than one.

[b] As by applying the EMF cut only jets originating in the calorimeters are considered, we do not need to apply an extrapolation of the jets to the calorimeter entry as described in the box about "Trigger Towers in MC Truth".

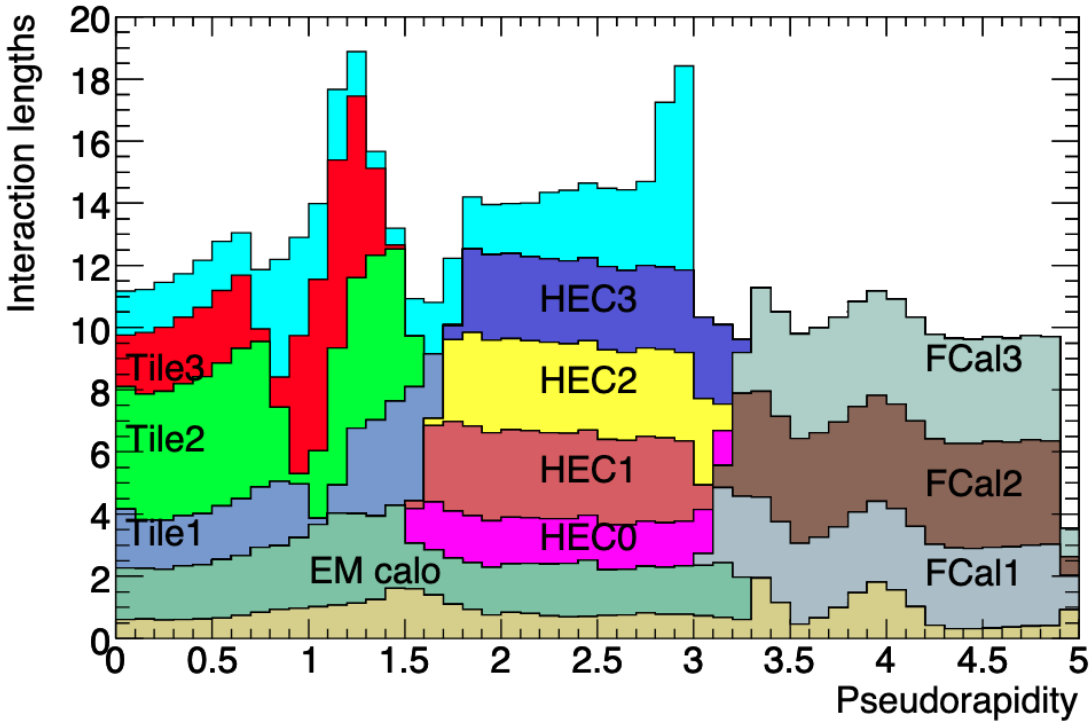

Figure 4: Material budget of the ATLAS detector in units of hadronic interaction length. Figure taken from [9].

High Level Trigger Decision of N in MC Truth (II)

$$\lambda_{\text{remaining}} = (\lambda_{\text{exit}} - \lambda_{\text{entry}}) \times \begin{cases} \dfrac{\rho_{\text{exit}} - \rho_0}{\rho_{\text{exit}} - \rho_{\text{entry}}} \\ \dfrac{z_{\text{exit}} - z_0}{z_{\text{exit}} - z_{\text{entry}}} \\ \dfrac{(1-\alpha)\left(\frac{\rho_{\text{exit}}-\rho_0}{\sin\theta}\right) + \alpha\left(\frac{z_{\text{exit}}-z_0}{\cos\theta}\right)}{(1-\alpha)\left(\frac{\rho_{\text{exit}}-\rho_{\text{entry}}}{\sin\theta}\right) + \alpha\left(\frac{z_{\text{exit}}-z_{\text{entry}}}{\cos\theta}\right)} \end{cases} \tag{13}$$

2. The jet is required to be isolated, i.e. there must not be tracks with $p_T > 2\,\text{GeV}$ in a $\Delta R = 0.2$ cone around the jet axis (which is defined based on equation 8). Tracks are defined as charged detector-stable truth particles with a production vertex in the inner detector and a readout time within the time window N; here, the readout time and (η, φ) coordinates are calculated based on the production vertex. Eventually, the isolation cut is applied by requiring $\Delta R > 0.2$ for all tracks with $p_T > 2\,\text{GeV}$.

3 Summary of changes w.r.t. previous selection cuts

- Previously, both the MET in $N-1$ as well as the jet in N were approximated by clustering the jets. While this was not too bad of an estimate for the jet in N, this approach significantly underestimated the MET in $N-1$. More precise algorithms to estimate the MET and jet

(similar to what is done in the hardware trigger) have been implemented. It was observed that the MET cut in $N-1$ now is less efficient by roughly a factor of 2.

- The fiducial and time cuts on the decays were tightened: previously, the timing cut was based on the decay time of the χ_1 particles, but the trigger actually does not know the decay time itself, but only the readout time, which is the decay time corrected by the "time of flight". This correction further separates the on- and out-of-time decays (on the exponential decay curve) which reduces the probability of decays in the desired time windows. Additionally, we introduced a selection cut on a maximal displacement in z direction of 5.5 m. Also the cut on the displacement in radial direction was tightened to 3.5 m (previously we used 4 m which sounds a bit too optimistic). Overall, the redefinition of the timing and fiducial cuts decrease the efficiency by a factor of 2.

- Alongside the new jet and MET algorithms, also the $\Delta\varphi$ cut is affected. Previously, a $\Delta\varphi$ of at least $\pi - 1.0$ was required for the two clustered higgs candidates, whereas now a maximal $\Delta\varphi$ of 1.0 between the MET and the jet is required. Furthermore, the φ coordinates are now calculated *in the calorimeter*, instead of using the clustered jet momenta.

- The high-level trigger decision has been implemented, which is pretty similar to what is used in the CalRatio analysis. This further reduces the number of events by a factor of 2.

Please note that the quoted efficiency factors are based on individual MC samples and are not necessarily representative of the entire phase space.

References

[1] **Extrapolation process:** https://gitlab.cern.ch/toheintz/l1-calo-llp-validation/-/blob/toheintz/L1algorithms/source/MCVal/Root/MCValAlg.cxx?ref_type=heads#L22-118

[2] **Trigger tower structure:** https://gitlab.cern.ch/toheintz/l1-calo-llp-validation/-/blob/toheintz/L1algorithms/source/MCVal/Root/MCValAlg.cxx?ref_type=heads#L1362-1462

[3] **Small R jet algorithm:** https://gitlab.cern.ch/toheintz/l1-calo-llp-validation/-/blob/toheintz/L1algorithms/source/MCVal/Root/MCValAlg.cxx?ref_type=heads#L1633-1831

[4] **MET algorithm:** https://gitlab.cern.ch/toheintz/l1-calo-llp-validation/-/blob/toheintz/L1algorithms/source/MCVal/Root/MCValAlg.cxx?ref_type=heads#L1471-1533

[5] **L1 Trigger decision:** https://gitlab.cern.ch/toheintz/edmgeneratorstudies/-/blob/L1algorithms/batch_scripts/trigger.py?ref_type=heads#L53-77

[6] **High-level trigger decision:** https://gitlab.cern.ch/toheintz/l1-calo-llp-validation/-/blob/toheintz/L1algorithms/source/MCVal/Root/MCValAlg.cxx?ref_type=heads#L1839-2020

[7] **Remaining interaction length:** https://gitlab.cern.ch/toheintz/l1-calo-llp-validation/-/blob/toheintz/L1algorithms/source/MCVal/Root/MCValAlg.cxx?ref_type=heads#L120-162

[8] https://doi.org/10.1051/epjconf/202024510003

[9] https://iopscience.iop.org/article/10.1088/1748-0221/3/08/S08003